

LASER: Tuning-Free LLM-Driven Attention Control for Efficient Text-conditioned Image-to-Animation

Haoyu Zheng Wenqiao Zhang Yaoke Wang Hao Zhou Jiang Liu

Juncheng Li Zheqi Lv Siliang Tang Yueting Zhuang

zhenghaoyu404@gmail.com, wenqiaozhang@zju.edu.cn, wangyaoke@zju.edu.cn, 2021210665@stu.hit.edu.cn
20201785@stu.cqu.edu.cn, junchengli@zju.edu.cn, zheqilv@zju.edu.cn, siliang@zju.edu.cn, yzhuang@zju.edu.cn

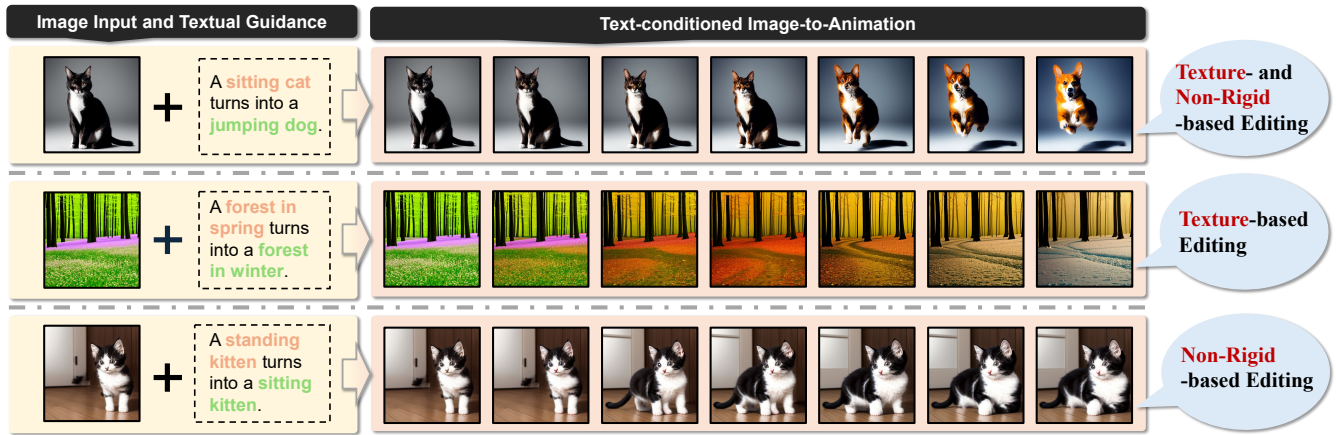


Figure 1: Given multimodal inputs (image and textual guidance), our method is capable of guiding the generation of smooth animations based on textual content. The first row shows the combined texture and non-rigid changes; the second row, only the texture changes; the third row, purely non-rigid transformations.

ABSTRACT

Revolutionary advancements in text-to-image models have unlocked new dimensions for sophisticated content creation, *e.g.*, text-conditioned image editing, allowing us to edit the diverse images that convey highly complex visual concepts according to the textual guidance. Despite promising, existing methods focus on texture- or non-rigid-based visual manipulation, which struggles to produce the fine-grained animation of the smooth text-conditioned image morphing without fine-tuning, *i.e.*, due to their highly unstructured latent space. In this paper, we introduce a tuning-free LLM-driven attention control framework, encapsulated by the progressive process of LLM planning \rightarrow prompt-Aware editing \rightarrow Stable animation geneRation, abbreviated as LASER: i) Given a general and coarse-grained description for image editing, LASER initially employs the large language model (LLM) that refines it into consistent and fine-grained prompts, which serve as linguistic guidance for the pre-trained text-to-image models in subsequent image generation; ii) We manipulate the model’s spatial features and self-attention mechanisms to maintain animation integrity and enable seamless image morphing directly from text prompts, obviating the need for annotations for additional fine-tuning; iii) Our meticulous control of spatial features and self-attention within the model ensures the preservation of structural consistency in the images. This paper introduces a novel framework that integrates large language models (LLM) with pre-trained text-to-image models to create high-quality image translation animations from just

one input text. The proposed LASER introduces a novel tuning-free framework that integrates LLM with pre-trained text-to-image models to facilitate high-quality text-conditioned image-to-animation translation. In addition, we propose a Text-conditioned Image-to-Animation Benchmark to validate the effectiveness and efficacy of the proposed LASER. Extensive experiments show that the proposed LASER produces impressive results in both consistent and efficient animation generation, positioning it as a powerful tool for producing detailed animations and opening new avenues in digital content creation.

CCS CONCEPTS

• Computing methodologies \rightarrow Computer vision.

KEYWORDS

Multimodal, Diffusion Model, Large Language Model

1 INTRODUCTION

Diffusion models [8, 12, 24] form a category of deep generative models that has recently become one of the hottest topics in multimodal intelligence, showcasing impressive capabilities of text-to-image (T2I) generation, ranging from the high level of details to the diversity of the generated examples. Such diffusion models also unlock a new world of creative processes in content creation, *e.g.*, text-guided image editing [5, 6, 10], involves editing the diverse images that convey highly complex visual concepts with text-to-image models

solely through the textual guidance. Broadly, the contemporary image editing paradigm can be summarized in two aspects: i) *Texture editing* [5, 6, 10], manipulating a given image’s stylization and appearance while maintaining the input structure and scene layout; ii) *Non-rigid Editing* [6, 18], enabling non-rigid image editing (e.g., posture changes) while preserving its original characteristics.

Despite achieving impressive image-level editing effects, the aforementioned methods fail to harness the editing animation, i.e., the smooth transition of the sequence of intermediary images according to the user’s textual requirement, including the fine-grained texture and non-rigid transformation. Such text-conditioned image-to-animation serves as an imperative component in various real-world content creation tasks, ranging from cinematic effects to computer games, as well as photo-editing tools for artistic and entertainment purposes to enrich people’s imagination. Nevertheless, realizing animation-level editing is highly challenging, primarily due to the highly unstructured latent space of the intermediary images. Of course, we can introduce more animation data to fine-tune the entire T2I diffusion models, thereby capturing the smooth animation edit. However, it comes at a tremendous cost and deteriorates the flexibility of the pre-trained diffusion models under the animation-level editing setting. Based on the above insights, one question is thrown: Given the input image and textual description, could we achieve the high-quality animation editing effect with the pre-trained text-to-image models without fine-tuning?

In this paper, we introduce a novel tuning-free LLM-driven attention control framework for text-conditioned image-to-animation, through LLM planing \rightarrow prompt-Aware Editing \rightarrow **Stable moR**phing, named as **LASER**. The core of our framework is that by leveraging the large language models (LLMs)[1, 21, 37, 48] with significant potential in natural language processing, to effectively parse the textual description into relevant and continuous control statements for pre-trained T2I diffusion models, thereby transforming the given image to animation. Specifically, LASER comprises the following progressive steps: **Step 1**, given a multi-modal input, i.e., a description of the animation P_0 and an initial image I_0 (which can be optional, allowing the T2I model generation), LLM decomposes the general and coarse-grained description P_0 into multiple fine-grained and consistent prompts. These prompts are closely aligned and exhibit subtle variations, aiding in the guided editing of subsequently corresponding keyframes; **Step 2**, the LLM analyzes these prompts to the feature and attention injection control signals, adapting to the nuanced differences between adjacent prompts. This enables tailored injection strategies for editing different keyframe types. Notably, the injection strategy delineates into two base categories: Feature and Association Injection (*FAI*) for texture-based editing and Key-Value Attention Injection (*KVAI*) for non-rigid editing. Notably, to facilitate the simultaneous portrayal of both texture and non-rigid editing within a singular animation phase, we propose the forward hybrid Attention Injection (*HAI*) for the image editing; **Step 3**, effectively synthesizing intermediate frames between keyframes, ensuring animations are coherent and fluid. This generator utilizes advanced interpolation methods, such as spherical linear interpolation, to ensure smooth transitions and reduce artifacts. Additionally, Adaptive Instance Normalization (*AdaIN*) is applied to enhance color and brightness consistency. The Hybrid Attention Injection (*HAI*) strategy is also employed

to integrate texture and structural transformations within a single animation phase, further enhancing the animation’s overall quality and coherence. Additionally, we inaugurate a Text-conditioned Image-to-Animation Benchmark, a comprehensive collection designed to challenge and quantify the adaptability and precision of the proposed LASER.

Summing up, our contributions can be concluded as:

- We introduce the tuning-free text-conditioned image-to-animation task, designed to craft high-quality animations based on the multimodal input using the pre-trained text-to-image models, without additional fine-tuning or annotations. To evaluate the efficacy of our approach, we introduce the *Text-conditioned Image-to-Animation Benchmark*, hoping that it may support future studies within this domain.
- The proposed the LASER encapsulated by the progressive process of LLM planing \rightarrow Prompt-aware editing \rightarrow Stable morphing, enabling the smooth texture- and non-rigid animation generation.
- Both qualitative and quantitative assessments underscore the superior efficacy of the proposed framework, showcasing its proficiency in generating animations that are not only smooth and of high quality but also diverse.

2 RELATED WORK

Text-to-Image Generation. In artificial intelligence[49–51], text-to-image (T2I) Generation aims to generate high-quality images based on text descriptions. Previous text-conditioned image generation approaches were primarily based on Generative Adversarial Networks (GANs) [4, 41, 43, 44, 52], leveraging their robust capabilities for high-fidelity image synthesis. These models, through multimodal vision-language learning, have endeavored to align text descriptions with synthesized image contents, yielding gratifying synthesis results on specific domain datasets. Recently, diffusion models [8, 12, 24] have demonstrated exceptional generative capabilities, achieving state-of-the-art results in terms of generation quality and diversity. By incorporating text prompts into diffusion models, various text-to-image diffusion models [28, 30, 31] have been developed. They are intricately conditioned on the provided text via cross-attention layers, ensuring that the generated images are not only visually coherent but also semantically consistent with the input descriptions.

Text-guided Image Editing. Text-guided image editing is a challenging task that aims to edit images based on textual descriptions, enabling users to achieve desired changes in natural language. Previous deep-learning-based approaches based on GANs [20, 23, 27, 40] have achieved certain success, but they are limited to specific domain datasets and exhibit limited applicability and generalization. VQGANCLIP [7] is an autoregressive model that combines VQGAN [9] and CLIP [29] to produce high-quality images and enable precise editing, yielding diverse and controllable results. However, this method suffers from slow generation speed and high computational cost. Recently, diffusion models trained on large-scale text-image pairs such as Imagen [31] and Stable Diffusion [30] have achieved unprecedented success in text-to-image generation. Therefore, they serve as a robust prior for various editing tasks, including text-guided image manipulation [5, 6, 10, 18, 26, 38]. Prompt-to-Prompt

[10] and Plug-and-Play [38] utilize cross-attention or spatial features to edit both global and local aspects of the image by directly modifying the text prompt. MasaCtrl [6] and Imagic [18] can handle non-rigid transformations such as changing object poses. Particularly, Plug-and-Play [38] consider the task of text-guided image-to-image translation that aims to estimate a mapping of an image from a source domain to a target domain, where the target domain is not specified through a dataset of images but rather via a target text prompt. However, most of these approaches directly generate the final edited image, with limited exploration concerning continuous animations such as image morphing.

Image Morphing. Image morphing is a task in computer graphics and image processing that aims to obtain reasonable intermediate images in the smooth transition between two images [2, 53]. With the advent of deep learning, neural networks have been used for image morphing, learning to identify correspondences and generate intermediate frames through latent interpolations. For instance, in the works on GANs [15–17, 32, 33], it has been demonstrated that their latent embedding space is highly continuous, and linear interpolation between two latent codes yields impressive image morphing results. Recent studies on diffusion models have also indicated the feasibility of generating plausible intermediate images through latent noise interpolation and text embedding interpolation [3, 36, 39]. Impus [42] explored the application of diffusion models in image morphing tasks, performing interpolation in the locally linear continuous text embedding space and Gaussian latent space. DiffMorpher [45] utilizes pre-trained diffusion models to achieve smooth and natural image interpolation and morphing. It performs spherical linear interpolation on the latent noise obtained through DDIM inversion for two images and combines it with text-conditioned linear interpolation, thus addressing the limitations of smooth interpolation between two image samples within the unstructured latent space of diffusion models.

3 METHODOLOGY

Given a user-defined descriptor P_* and an initial image I_0 (provided or generated), our method generates the animation sequence $\{x_0^{(\alpha)}, x_1^{(\alpha)}, \dots, x_n^{(\alpha)}\}$, where α varies from 0 to 1. The length of the $x_i^{(\alpha)}$ sequence is set by n_f and the number of sequences $x_i^{(\alpha)}$ corresponds to the transformation stages n_t . The resulting animation is expected to visually manifest the smooth transitions of I_0 to I_n and characteristics as described by P_* . To guide this generative process, a series of descriptive prompts $\{P_0, P_1, \dots, P_{n_t}\}$ are derived to anchor each keyframe in the animation’s continuity.

3.1 Preliminary for Diffusion Models

Diffusion models [12] [35] [24] are a series of probabilistic generative models that produce images by gradual denoising from a noise distribution, e.g., Gaussian distribution. The generation process consists of two main phases: the *forward* (diffusion) process and *reverse* (denoising) process.

The *forward* process gradually adds noise to initial data x_0 to generate a noisy data x_t given variance schedule $\alpha_t \in (0, 1)$ at time-step t :

$$q(x_t|x_0) = \mathcal{N}(x_t; \sqrt{\bar{\alpha}_t}x_0, (1 - \bar{\alpha}_t)\mathbf{I}), \quad (1)$$

where $\bar{\alpha}_t = \prod_{i=1}^t \alpha_i$. After T steps, we obtain noise $x_T \sim \mathcal{N}(0, 1)$.

The *reverse* process aims to gradually clean the noise. By utilizing the Bayzes’ rules and Markov property, we can intuitively express the conditional probabilities as:

$$q(x_{t-1}|x_t) = \mathcal{N}(x_{t-1}; \frac{1}{\sqrt{\alpha_t}}(x_t - \frac{1 - \alpha_t}{\sqrt{1 - \bar{\alpha}_t}}\epsilon), \tilde{\beta}_t\mathbf{I}), \quad (2)$$

where $\tilde{\beta}_t$ is a time-dependent constant and added noise ϵ can be predicted by a neural network ϵ_θ . By sampling x_{t-1} iteratively, we finally get a clean image x_0 from initial Gaussian noise x_T .

We employ a text-conditioned Stable Diffusion (SD) [30], which operates within lower-dimensional latent space rather than pixel space. It begins with encoding images to latent representation by a variational auto-encoder (VAE) [19], followed by a diffusion-denoising process within the latent space. After denoising, the latent representation is decoded back into the image space via a decoder network, culminating in the final generated image.

In the noise-predicting network ϵ_θ , residual blocks process image features to generate intermediate features f_t^l , which are then used in the self-attention module to produce Q, K, V for capturing long-range interactions. Subsequently, cross-attention integrates textual prompt P input, merging text and image semantics. The attention mechanism can be formulated as follows:

$$Attention(Q, K, V) = softmax(\frac{QK^T}{\sqrt{d_k}})V, \quad (3)$$

where Q, K , and V represent queries, keys, and values, respectively, with d_k denoting the key/query dimension for scaling dot product. In this model, Q originates from spatial features, while K and V come from spatial features and text embeddings for self and cross-attention, respectively. Leveraging attention layers within the SD model significantly affects image composition and development [10] [38], guiding image editing and synthesis by manipulating attention-related information during denoising [6].

3.2 LLM-driven Controller

In this section, we first utilize LLM to extract aligned textual prompts for each key animation stage. Our approach supports two input modalities: text-image pairs and text-only inputs. If the user provides an image, it is directly utilized as the initial image I_0 . In cases where the initial image is absent, we leverage pre-trained Stable Diffusion models to generate I_0 . To generate animations that adhere to the semantics of a specified text description P_* , we require text prompts $\{P_0, P_1, \dots, P_{n_t}\}$ for each key animation stage, as these prompts directly guide the animation process. High-quality, detailed text prompts are crucial when no initial image is provided, as the model generates I_0 based on P_0 ’s semantic cues. Prompts for Stable Diffusion should be richly descriptive to accurately produce a high-quality starting image.

To enhance the quality and stability of the process, we introduce two agents based on large language models: the “Stage Image Text Prompt Agent” (SIA) and the “Stable Diffusion Prompt Generator Agent” (PGA). Initially, SIA generates text prompts that guide the image generation for each key stage, as illustrated in Fig. 2 (a). SIA generates text prompts based on two fundamental principles: i) By decomposing the animation descriptor P_* into multiple independent processes, SIA reduces semantic differences between

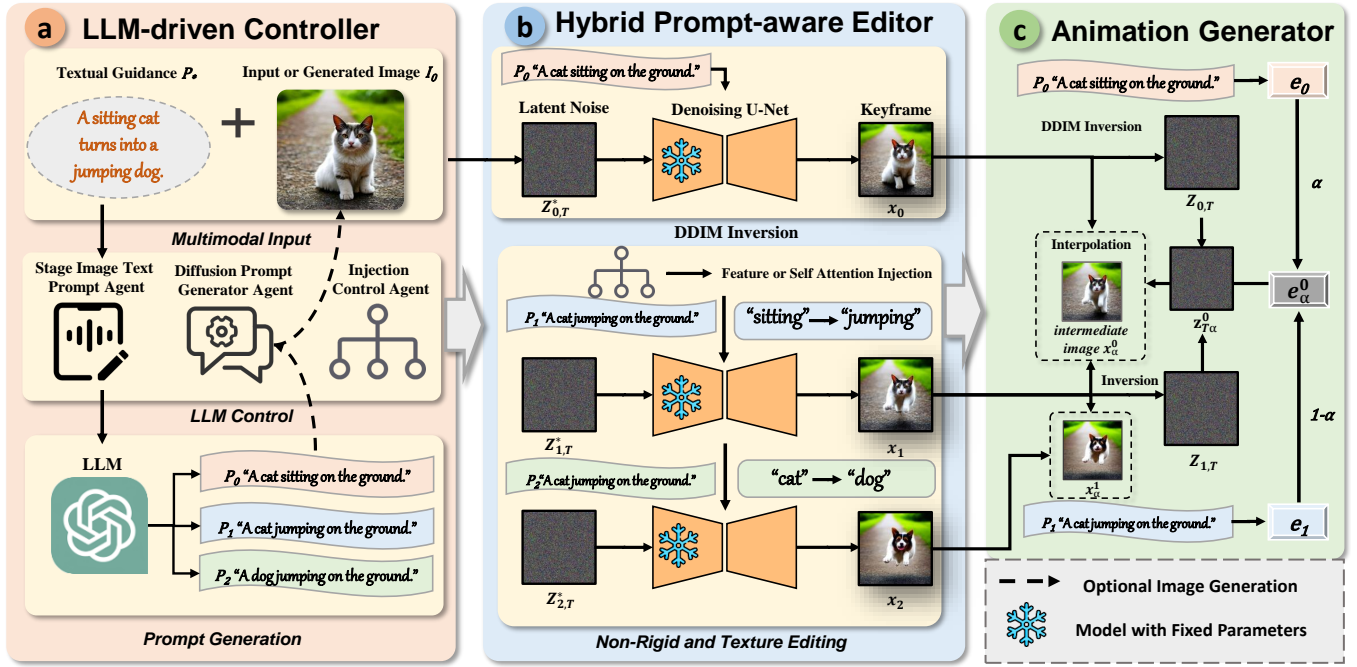


Figure 2: Overview of proposed LASER. (a) The LLM-driven Controller first parses the descriptive prompts to generate the descriptive prompts for corresponding frames of animation. (b) By doing so, the LLM analyzes these prompts to the feature and attention injection control signals, to facilitate the simultaneous portrayal of both texture and non-rigid editing. (c) The animation generator leverages spherical linear interpolation and adaptive instance normalization to generate the intermediate images between keyframes, accessing smooth animation generation.

adjacent prompts, enhancing the overall quality of the results. ii) The prompts must be highly aligned to facilitate high-quality intermediate results through linear interpolation. Given the local linearity within the CLIP text embedding space [18], minimizing the gap between adjacent embeddings is essential. A practical method involves using consistent sentence structures across prompts, such as “A cat [action] on the ground” and “A [animal] jumping on the ground” [42]. This approach ensures that while the prompts are semantically distinct, they share a common categorical root, thus streamlining the generation process. This generation method successfully mitigates the non-linearity and discontinuity commonly encountered between text embeddings. With the deployment of the Stage Image Text Prompt Agent (SIA), we significantly bolster our model’s capacity to generate semantically coherent and high-quality images. The Stable Diffusion Prompt Generator Agent (PGA) converts broad, high-level concepts from the SIA into richly detailed and vividly descriptive prompts specifically crafted for Stable Diffusion. As depicted in Fig. 2 (b), once PGA receives the initial text prompt from SIA, it refines this input to craft a more detailed prompt. This enhanced prompt not only delineates the subject and action but also enriches the scene with specific elements like texture, lighting, and artistic style, which instructs Stable Diffusion to produce images of higher fidelity and complexity [22].

3.3 Hybrid Prompt-aware Editor

This section utilizes the aligned textual prompts to obtain keyframe images. During the editing process, $Z_{1,T}^*$ is a direct copy of $Z_{0,T}^*$. For $i \geq 1$, each keyframe x_i undergoes DDIM inversion to produce $Z_{i,T}$, which is then cloned to form $Z_{i+1,T}^*$ for the subsequent keyframe. Despite using aligned prompts for text-guiding image editing, we still observe a marked discrepancy in semantic identity between the images, which results in animations that do not transition smoothly. To overcome this challenge, we draw inspiration from previous image editing techniques [6, 38] and propose a feature and attention injection method controlled by the LLM, tailored to query semantically similar content from the previous keyframes according to the changing nature of the corresponding stage.

Utilizing DDIM inversion on the prior keyframe, we obtain the initial state $Z_{i,T}$. Past work [38] has demonstrated that injecting features f_t^l within residual blocks and self-attention projections q_t^l , k_t^l significantly boosts text-guided image editing tasks. The encoding in the fourth layer f_t^4 specifically captures shared semantics necessary for structure retention during generation. Moreover, the injections of self-attention are underpinned by the attention scores, which arise from the product of query and key vectors, exhibiting a profound connection to the well-established self-referential paradigms within neural attention schemas. By injecting specific features f_t^4 into the fourth layer of residual blocks and introducing self-attention elements q_t^l and k_t^l throughout all decoder layers, we have successfully achieved texture variations between keyframes.

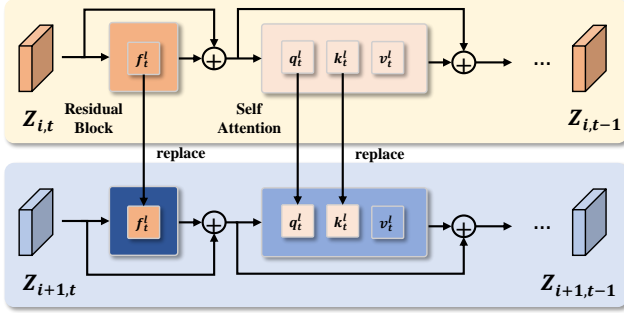


Figure 3: Overview of Feature and Association Injection.

We refer to this injection strategy as “Feature and Association Injection” (FAI).

However, the aforementioned method struggles with non-rigid keyframe modifications. The usual solution, limiting injection range to reflect rigid changes from prompts, risks losing image identity. To navigate this, especially for non-rigid edits, we avoid injecting into residual blocks, thereby maintaining the image’s structural integrity without being obscured by local semantics. Our strategy uses targeted attention injections. As image layout solidifies early in denoising and self-attention queries align semantically [6], they can extract content from various objects. Post-denoising, we inject keys k_i^l and values v_i^l from the previous keyframe’s self-attention block, as shown in Fig. 4. This process forms objects’ outlines following text prompts and then enriches the generative structure with detailed content from the source image. Consequently, we achieve semantically coherent images that also support non-rigid transitions. We refer to this injection strategy as “Key-Value Attention Injection” (KVAI). Up to this point, the model has acquired the capability to generate diverse keyframes, enabling the production of the expected animations.

Recognizing the need for a systematic approach to select the optimal injection strategy for each stage of the animation generation, we have developed the *Injection Control Agent* (ICA), as showcased in Fig. 2 (a). ICA’s primary role is to process the text prompts from the Stage Image Text Prompt Agent (SIA), which performs an in-depth analysis of semantic differences between these text prompts at consecutive key stages. This analysis enables SIA to issue tailored control signals: “0” signals ICA to deploy the injection strategy for stages where texture changes are dominant, and “1” signals the use of the KVAI strategy for stages with non-rigid transformations. By precisely managing the type of attention injection at each stage, ICA ensures that the generated animations are both visually coherent and closely aligned with the textual descriptors.

3.4 Animation Generator

In this section, we generate intermediate images between keyframe images to obtain consistent and smooth animations. After generating the text prompts corresponding to each key stage P_0, P_1, \dots, P_{n_t} in section 3.2, we obtain the respective text embeddings e_0, e_1, \dots, e_{n_t} . When generating intermediate images, we perform a simple linear interpolation between the text embeddings of two adjacent key stages to obtain the corresponding text embedding e .

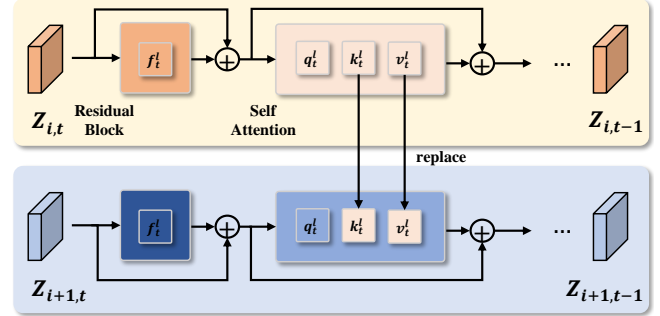


Figure 4: Overview of Key-Value Attention Injection.

$$e_\alpha^i = (1 - \alpha)e_i + \alpha e_{i+1} \quad (4)$$

In the construction of the animation sequence, the interpolation parameter α is discretized into a series of values that facilitate a smooth transition between frames. This discretization is achieved by defining a set of equidistant points within the closed interval $[0, 1]$, where the number of points corresponds to the intended number of frames in an animation stage, denoted as n_f . Thus, α takes on values $\alpha_0, \alpha_1, \dots, \alpha_{n_f-1}$, where $\alpha_0 = 0$ represents the starting frame, and $\alpha_{n_f-1} = 1$ indicates the ending frame. The intermediate values of α correspond to proportionally spaced frames within the animation sequence, ensuring linear spacing. This arrangement guarantees that each frame represents a weighted blend of the preceding and subsequent key stage embeddings, facilitating a smooth and continuous transformation across the animation.

To ensure visual continuity in the sequence of intermediate images, we interpolate the latent noise of these images using the latent noise from adjacent key stages. However, standard linear interpolation may introduce artifacts. To address this, we adopt spherical linear interpolation (slerp) [34], which effectively minimizes artifacts and enhances the smoothness of transitions.

$$z_{T\alpha}^i = \frac{\sin((1 - \alpha)\xi)}{\sin \xi} z_{i,T} + \frac{\sin(\alpha\xi)}{\sin \xi} z_{i+1,T} \quad (5)$$

$$\text{where } \xi = \arccos\left(\frac{z_{i,T} \cdot z_{i+1,T}}{\|z_{i,T}\| \|z_{i+1,T}\|}\right).$$

To maintain consistency in the color and luminance aspects of both generated and source images, we implement a variant of Adaptive Instance Normalization (AdaIN) [14] for the pre-denoising stage adjustment of the interpolated latent noise $z_{0\alpha}^i$. We calculate and then interpolate the means (μ) and standard deviations (σ) of the latent noises for each channel:

$$\mu_\alpha^i = (1 - \alpha)\mu_i + \alpha\mu_{i+1} \quad (6)$$

$$\sigma_\alpha^i = (1 - \alpha)\sigma_i + \alpha\sigma_{i+1} \quad (7)$$

$$\tilde{z}_{0\alpha}^i = \sigma_\alpha^i \left(\frac{z_{0\alpha}^i - \mu(z_{0\alpha}^i)}{\sigma(z_{0\alpha}^i)} \right) + \mu_\alpha^i \quad (8)$$

Subsequently, adjusted latent noise $\tilde{z}_{0\alpha}^i$ supplants the original $z_{0\alpha}^i$ during the denoising steps, thereby improving the brightness and color consistency of the resulting images.



Figure 5: Qualitative evaluation. Our method produces animations that significantly outperform previous methods in terms of quality, smoothness, and alignment with user input.

Finally, during the denoising process of each intermediate image x_α^i , we also perform feature and self-attention injection. When the stage number n_t is not “-1”, we implement the standard injection strategy, wherein, while generating x_α^i , the injection is obtained from x_i . Furthermore, when SLA’s feedback on the “ n_t ” is “-1”, it indicates a special request from the user for a “single-stage generation,” which involves both texture changes and non-rigid transformations within a single animation stage. In such cases, ICA leads the model to execute the Hybrid Attention Injection (HAI) strategy. HAI solves the issue that when using the normal injection strategies, the model is unable to produce animations that simultaneously exhibit changes in texture and structure within a single phase. This phenomenon will be further discussed in the 4. The HAI process initiates by editing x_0 to produce x_1 using the Feature and Association Injection (FAI), and subsequently x_2 is edited from x_1 utilizing the KVAI. Following these edits, DDIM Inversion is applied to extract the latent representations $Z_{0,T}$ and $Z_{2,T}$, which are then interpolated to construct the intermediate latent representation $z_{T\alpha}^i$. During the denoising phase, injections are strategically administered based on the interpolation parameter α ; specifically, injections from $\{k_t^i, v_t^i\}$ corresponding to x_0 are applied in the initial $(1-\alpha)T$ steps, and those corresponding to x_2 in the subsequent αT steps. This method effectively conveys the semantic and structural information of significantly transformed images, ensuring smooth

and consistent animations by querying local structures and textures from input images throughout the denoising process.

4 EXPERIMENTS

We employ the publicly available Stable Diffusion v2.1-base [30] as our diffusion model and use GPT-4 8k [25] as the LLM in our experiments. For generating the initial image I_0 , we utilize two pre-trained models: the real-style model dreamshaper-8 and the anime-style model MeinaMix, to assess our model’s capability in producing animations across diverse styles. In creating intermediate images, we apply DDIM deterministic sampling. For keyframe synthesis, aiming to optimize the balance between efficiency and quality, we perform deterministic DDIM inversion with 100 forward steps followed by deterministic DDIM sampling with 100 backward steps. When implementing Feature and Association Injection (FAI), we inject features and self-attention within the first 25 of the 50-step sampling process, specifically targeting layers 4 to 10 of the U-Net decoder. In the case of Key-Value Attention Injection (KVAI), injections commence after the initial five sampling steps and are applied within layers 6 to 10 of the decoder. The Hybrid Attention Injection (HAI) method follows the same timing and targets the same layers as KVAI. These injection strategies can be customized to align with the different input images I_0 . For sampling, the classifier-free guidance scale is set at 7.5. Runtime evaluations are performed on an NVIDIA RTX 4090 GPU.

4.1 Text-conditioned Image-to-Animation Benchmark

Our method enables text-guided image-to-animation transitions, leveraging either image-textual or solely textual descriptions through pre-trained text-to-image diffusion models. Due to the lack of benchmarks for such configurations, we have proposed a new mini dataset: *Text-conditioned Image-to-Animation Benchmark*, which consists of 100 sets of textual descriptions. The collection comprises 100 sets, categorized as follows: 20 sets of animal actions and appearance transformations, 20 sets focused on animal appearance and species changes, 20 sets depicting transitions in natural landscapes and objects, 20 sets related to human figures and alterations in painting styles, 10 sets featuring character identity transformations, and 10 sets concerning changes in object colors and materials. Our model utilizes these textual prompts to generate 100 corresponding animation sequences. This benchmark serves as a preliminary evaluation of our model’s performance, and we hope it will facilitate further research in this direction.

4.2 Qualitative Evaluation

We present a visual comparison of our method against prior approaches to underscore its superiority. Although there are no other tuning-free methods for text-controlled image-to-animation currently available, we draw a detailed comparison with state-of-the-art baselines promising for text-controlled image morphing. These include: 1) Diffusion-based deep interpolation methods such as DDIM [35], Diff.Interp [39], and DiffMorpher [45], all utilizing Stable Diffusion v2.1-base; 2) Text-driven, tuning-free image editing methods like PnP [38] and MasaCtrl [6]. For the first category of methods, which depend on multiple pre-existing image inputs and lack the capability to generate content directly from text, our experimental procedure includes: i) Utilizing LLM control for generating consistent outputs, which involves creating initial images and key stage prompts through stable diffusion prompt generation, similar to our method. ii) Generating initial images using the same stable diffusion checkpoint as employed in our experiments. iii) Producing subsequent key stage images via DDIM Inversion. For the second category, which also leverages LLM control, we maintain consistent application of text embedding interpolation rules to generate intermediate images, aligning with our approach.

Generation Results. As illustrated in Fig. 5, our method outperforms previous approaches in alignment with user input, transition smoothness, semantic coherence, and maintaining the animation subject’s semantic identity. Previous methods have often failed to accurately respond to user input changes in appearance and motion. These approaches typically struggle to generate the intended motions accurately or introduce noticeable artifacts post-motion changes, often resulting in a significant loss of primary subject information in the images. Compared to previous methods, our approach consistently generates coherent animations that closely align with the semantic content of the user input, resulting in visually satisfactory outputs. For additional examples of generated results, we encourage readers to consult the appendix.

Generation Diversity. Furthermore, the extensive prior knowledge and generative capabilities of the LLM enhance our model’s

ability to produce diverse outputs, as shown in Fig. 6. When users request multiple distinct results, our model meets this demand by generating high-quality, varied animations, significantly broadening its creative potential.

4.3 Quantitative Evaluation

Drawing from established objectives in prior research [6, 42, 45], we quantitatively evaluate the models using these metrics:

- (1) Learned Perceptual Image Patch Similarity (LPIPS, ↓) [47]: LPIPS is employed to assess the perceptual deviation within an animation sequence in our work. We compute the total LPIPS ($LPIPS_T$) to quantify the overall perceptual variance throughout the sequence, highlighting the dynamic range of visual changes. Additionally, the maximum LPIPS to the nearest endpoint ($LPIPS_M$) is determined to identify the maximum perceptual variance, providing insights into the most significant changes within the animation. These measurements are crucial for assessing directness of the animation, ensuring finding the most efficient transition to generate animation.
- (2) CLIP Score (↑) [11]: The CLIP score is a metric that quantifies the alignment between images and textual descriptions, serving as a powerful tool for evaluating the coherence and relevance of generated images about their specified textual prompts. For an intermediate image, we describe its CLIP score by calculating its average similarity with the prompt before editing and the prompt after editing (e.g., x_α^0 with P_0 and P_1 , x_α^1 with P_1 and P_2 , etc.).
- (3) Perceptual Path Length (PPL, ↓) [17]: To evaluate smoothness, i.e., transitions within the generated animation sequence should be seamless between any two consecutive images, we compute **PPL**: $PPL_\epsilon = \mathbb{E}_{\alpha \sim U(0,1)} [\frac{1}{\epsilon^2} LPIPS(x^{(\alpha)}, x^{(\alpha+\epsilon)})]$, where ϵ is a small constant and we set it to $\frac{1}{n_f-1}$. It is worth noting that we regard the entire sequence as a single animation process, despite consisting of multiple stages.

The quantitative evaluation results of all methods are presented in Table 1.

Generation Quality. Our method achieves a leading Clip Score, demonstrating its semantic alignment with user input. While DDIM may excel in CLIP Score, it often compromises structural coherence in favour of textual alignment, an issue our approach adeptly avoids as demonstrated in Fig. 5. Due to PnP’s inability to effectively perform non-rigid edits, its generated animations often exhibit only appearance changes, thereby achieving higher levels of smoothness. This limitation hinders its capability to handle a diverse range of animation generation tasks. Similarly, Masacontrol, which struggles with texture transformations, also falls short in producing a diverse range of animations. Even when benchmarked against deep interpolation techniques that require fine-tuning, our results consistently exhibit superior smoothness. This performance not only underscores the effectiveness of our method but also affirms its suitability for adapting to a wide range of text-conditioned image-to-animation generation scenarios.



Figure 6: The rich prior knowledge of the LLM grants the model the ability to generate diverse outcomes from the same input text and image.

Table 1: Comparison of current methods. Superscript ^{*} indicates that the model employs an external network (e.g., ControlNet [46]) to generate intermediate images and [†] indicates that the model fine-tunes with training LoRA [13]. "TE" stands for texture editing, a process that involves altering the surface appearance of objects within an image to match a specific texture style, while preserving the underlying structure and layout of the scene. "NRIE" refers to non-rigid image editing which involves altering the shape and structure of objects in images, like changing facial expressions or body poses. "AG", standing for animation generation, refers to producing intermediate images between keyframes.

Method	Characteristics			Metrics				Runtime↓
	TE	NRIE	AG	CLIP Score ↑	LPIPS _T ↓	LPIPS _M ↓	PPL ↓	
DDIM[35]	✓			27.37	3.13	0.49	36.91	32s
PnP[10]	✓			26.57	0.90	0.23	10.51	2min
MasaCtrl[6]		✓		26.56	1.54	0.28	17.96	37s
Diff.Interp [*] [39]			✓	20.05	5.14	0.58	72.29	2min6s
DiffMorpher [†] [45]		✓	✓	26.94	0.99	0.40	14.78	1min46s
Ours	✓	✓	✓	26.99	1.22	0.25	14.14	41s

Generation Efficiency. In assessing efficiency, our method uniquely blends quality with speed, setting it apart from other deep interpolation techniques. This superior performance primarily stems from our operation without the need for fine-tuning. Although it may not lead in all image editing benchmarks, our model excels at managing a diverse array of edits, enabling it to adeptly tackle a broad spectrum of generative tasks. Given this versatility, the efficiency of our method is exceptionally high.

4.4 Ablation Study

We have conducted an ablation study to evaluate the effectiveness of the proposed components, with experimental results shown in Table 2 and Fig.2 (in Appendix). The findings demonstrate that using DDIM alone cannot accurately restore the structure of the input image. In contrast, our feature and self-attention injections address the loss of texture and structural information during the DDIM generation process, significantly enhancing the quality of the generated animations. However, remnants of structural features from the initial state are still noticeable in the generated animations, including in the intermediate segments. The implementation of Latent Interpolation addresses this issue. While it may slightly

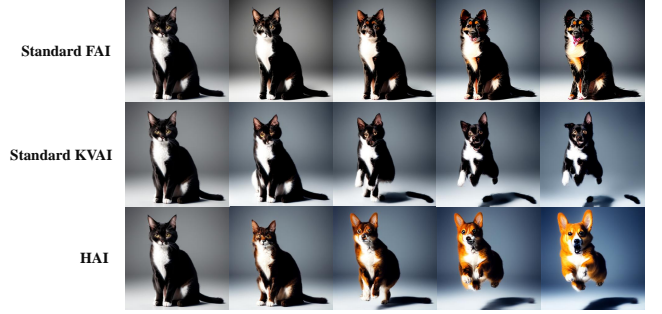


Figure 7: The comparative effects of different injection strategies given the textual description "A sitting cat turns into a jumping dog".

Table 2: Ablation study results. Injection, Latent Interp, and AdaIN represent different components studied in the ablation.

Method	Components			Metrics			
	Injection	Latent Interp	AdaIN	Clip Score ↑	LPIPS _T ↓	LPIPS _M ↓	PPL ↓
DDIM[35]				27.37	3.13	0.49	36.91
-	✓			26.73	1.09	0.26	12.85
-	✓	✓		26.81	1.22	0.26	14.03
Ours	✓	✓	✓	26.99	1.22	0.25	14.14

elevate the $LPIPS_T$ and PPL metrics, it ensures that subsequent frames more accurately reflect the semantic information of the transformed state. After applying the AdaIN adjustment to the latent noise, the consistency of brightness and color across the image sequence has improved.

To demonstrate the effectiveness of Hybrid Attention Injection (HAI) in producing single-stage animations that incorporate both texture changes and non-rigid transformations, we conducted qualitative experiments. We generated animations using basic injection strategies (FAI and KVAI) and HAI, with the results displayed in Fig. 7. When employing only FAI, the images failed to respond to non-rigid changes; using KVAI alone did not result in significant texture modifications. Our proposed HAI strategy successfully handles both texture and non-rigid changes, effectively fulfilling the task of single-stage animation generation.

5 CONCLUSION

We introduce LASER, a tuning-free LLM-driven attention control framework that utilizes pre-trained text-to-image models to generate high-quality and smooth animations from multimodal inputs. Experimental results validate the superior performance of our method, which consistently produces diverse and high-quality animations. We believe our approach demonstrates significant potential and serves as an inspiration for future research in this field.

REFERENCES

- [1] Josh Achiam, Steven Adler, Sandhini Agarwal, Lama Ahmad, Ilge Akkaya, Florencia Leoni Aleman, Diogo Almeida, Janko Altenschmidt, Sam Altman, Shyamal Anadkat, et al. 2023. Gpt-4 technical report. *arXiv preprint arXiv:2303.08774* (2023).
- [2] Alyaa Qusay Aloraibi. 2023. Image morphing techniques: A review. (2023).
- [3] Fan Bao, Shen Nie, Kaiwen Xue, Chongxuan Li, Shi Pu, Yaole Wang, Gang Yue, Yue Cao, Hang Su, and Jun Zhu. 2023. One transformer fits all distributions in multi-modal diffusion at scale. In *International Conference on Machine Learning*. PMLR, 1692–1717.
- [4] Andrew Brock, Jeff Donahue, and Karen Simonyan. 2018. Large scale GAN training for high fidelity natural image synthesis. *arXiv preprint arXiv:1809.11096* (2018).
- [5] Tim Brooks, Aleksander Holynski, and Alexei A Efros. 2023. Instructpix2pix: Learning to follow image editing instructions. In *Proceedings of the IEEE/CVF Conference on Computer Vision and Pattern Recognition*. 18392–18402.
- [6] Mingdeng Cao, Xintao Wang, Zhongang Qi, Ying Shan, Xiaoju Qie, and Yinqiang Zheng. 2023. Masactrl: Tuning-free mutual self-attention control for consistent image synthesis and editing. In *Proceedings of the IEEE/CVF International Conference on Computer Vision*. 22560–22570.
- [7] Katherine Crowson, Stella Biderman, Daniel Kornis, Dashiell Stander, Eric Hallahan, Louis Castricato, and Edward Raff. 2022. Vqgan-clip: Open domain image generation and editing with natural language guidance. In *European Conference on Computer Vision*. Springer, 88–105.
- [8] Prafulla Dhariwal and Alexander Nichol. 2021. Diffusion models beat gans on image synthesis. *Advances in neural information processing systems* 34 (2021), 8780–8794.
- [9] Patrick Esser, Robin Rombach, and Bjorn Ommer. 2021. Taming transformers for high-resolution image synthesis. In *Proceedings of the IEEE/CVF conference on computer vision and pattern recognition*. 12873–12883.
- [10] Amir Hertz, Ron Mokady, Jay Tenenbaum, Kfir Aberman, Yael Pritch, and Daniel Cohen-Or. 2022. Prompt-to-prompt image editing with cross attention control. *arXiv preprint arXiv:2208.01626* (2022).
- [11] Jack Hessel, Ari Holtzman, Maxwell Forbes, Ronan Le Bras, and Yejin Choi. 2021. Clipscore: A reference-free evaluation metric for image captioning. *arXiv preprint arXiv:2104.08718* (2021).
- [12] Jonathan Ho, Ajay Jain, and Pieter Abbeel. 2020. Denoising diffusion probabilistic models. *Advances in neural information processing systems* 33 (2020), 6840–6851.
- [13] Edward J Hu, Yelong Shen, Phillip Wallis, Zeyuan Allen-Zhu, Yuanzhi Li, Shean Wang, Lu Wang, and Weizhu Chen. 2021. Lora: Low-rank adaptation of large language models. *arXiv preprint arXiv:2106.09685* (2021).
- [14] Xun Huang and Serge Belongie. 2017. Arbitrary style transfer in real-time with adaptive instance normalization. In *Proceedings of the IEEE international conference on computer vision*. 1501–1510.
- [15] Tero Karras, Miika Aittala, Samuli Laine, Erik Härkönen, Janne Hellsten, Jaakko Lehtinen, and Timo Aila. 2021. Alias-free generative adversarial networks. *Advances in neural information processing systems* 34 (2021), 852–863.
- [16] Tero Karras, Samuli Laine, and Timo Aila. 2019. A style-based generator architecture for generative adversarial networks. In *Proceedings of the IEEE/CVF conference on computer vision and pattern recognition*. 4401–4410.
- [17] Tero Karras, Samuli Laine, Miika Aittala, Janne Hellsten, Jaakko Lehtinen, and Timo Aila. 2020. Analyzing and improving the image quality of stylegan. In *Proceedings of the IEEE/CVF conference on computer vision and pattern recognition*. 8110–8119.
- [18] Bahjat Kawar, Shiran Zada, Oran Lang, Omer Tov, Huiwen Chang, Tali Dekel, Inbar Mosseri, and Michal Irani. 2023. Imagic: Text-based real image editing with diffusion models. In *Proceedings of the IEEE/CVF Conference on Computer Vision and Pattern Recognition*. 6007–6017.
- [19] Diederik P Kingma and Max Welling. 2013. Auto-encoding variational bayes. *arXiv preprint arXiv:1312.6114* (2013).
- [20] Bowen Li, Xiaojuan Qi, Thomas Lukasiewicz, and Philip HS Torr. 2020. Manigan: Text-guided image manipulation. In *Proceedings of the IEEE/CVF conference on computer vision and pattern recognition*. 7880–7889.
- [21] Juncheng Li, Kaihang Pan, Zhiqi Ge, Minghe Gao, Wei Ji, Wenqiao Zhang, Tat-Seng Chua, Siliang Tang, Hanwang Zhang, and Yueting Zhuang. 2023. Fine-tuning multimodal llms to follow zero-shot demonstrative instructions. In *The Twelfth International Conference on Learning Representations*.
- [22] Long Lian, Boyi Li, Adam Yala, and Trevor Darrell. 2024. LLM-grounded Diffusion: Enhancing Prompt Understanding of Text-to-Image Diffusion Models with Large Language Models. *arXiv:2305.13655 [cs.CV]*
- [23] Seonghyeon Nam, Yunji Kim, and Seon Joo Kim. 2018. Text-adaptive generative adversarial networks: manipulating images with natural language. *Advances in neural information processing systems* 31 (2018).
- [24] Alexander Quinn Nichol and Prafulla Dhariwal. 2021. Improved denoising diffusion probabilistic models. In *International conference on machine learning*. PMLR, 8162–8171.
- [25] OpenAI, Josh Achiam, Steven Adler, Sandhini Agarwal, Lama Ahmad, Ilge Akkaya, Florencia Leoni Aleman, Diogo Almeida, Janko Altenschmidt, Sam Altman, Shyamal Anadkat, Red Avila, Igor Babuschkin, Suchir Balaji, Valerie Balcom, Paul Baltescu, Haiming Bao, Mohammad Bavarian, Jeff Belgum, Irwan Bello, Jake Berdine, Gabriel Bernadett-Shapiro, Christopher Berner, Lenny Boudeno, Oleg Boiko, Madelaine Boyd, Anna-Luisa Brakman, Greg Brockman, Tim Brooks, Miles Brundage, Kevin Button, Trevor Cai, Rosie Campbell, Andrew Cann, Brittany Carey, Chelsea Carlson, Rory Carmichael, Brooke Chan, Che Chang, Fotis Chantzis, Derek Chen, Sully Chen, Ruby Chen, Jason Chen, Mark Chen, Ben Chess, Chester Cho, Casey Chu, Hyung Won Chung, Dave Cummings, Jeremiah Currier, Yunxing Dai, Cory Decareaux, Thomas Degry, Noah Deutsch, Damien Deville, Arka Dhar, David Dohan, Steve Dowling, Sheila Dunning, Adrien Ecoffet, Atty Eleti, Tyna Eloundou, David Farhi, Liam Fedus, Niko Felix, Simón Posada Fishman, Juston Forte, Isabella Fulford, Leo Gao, Elie Georges, Christian Gibson, Vik Goel, Tarun Gogineni, Gabriel Goh, Rapha Gontijo-Lopes, Jonathan Gordon, Morgan Grafstein, Scott Gray, Ryan Greene, Joshua Gross, Shixiang Shane Gu, Yufei Guo, Chris Hallacy, Jesse Han, Jeff Harris, Yuchen He, Mike Heaton, Johannes Heidecke, Chris Hesse, Alan Hickey, Wade Hickey, Peter Hoeschele, Brandon Houghton, Kenny Hsu, Shengli Hu, Xin Hu, Joost Huizinga, Shantanu Jain, Shawn Jain, Joanne Jang, Angela Jiang, Roger Jiang, Haozhun Jin, Denny Jin, Shino Jomoto, Billie Jonn, Heewoo Jun, Tomer Kaftan, Lukasz Kaiser, Ali Kamali, Ingmar Kanitscheider, Nitish Shirish Keskar, Tabarak Khan, Logan Kilpatrick, Jong Wook Kim, Christina Kim, Yongjik Kim, Jan Hendrik Kirchner, Jamie Kiros, Matt Knight, Daniel Kokotajlo, Łukasz Kondraciuk, Andrew Kondrich, Aris Konstantinidis, Kyle Kopic, Gretchen Krueger, Vishal Kuo, Michael Lampe, Ikai Lan, Teddy Lee, Jan Leike, Jade Leung, Daniel Levy, Chak Ming Li, Rachel Lim, Molly Lin, Stephanie Lin, Mateusz Litwin, Theresa Lopez, Ryan Lowe, Patricia Lue, Anna Makanju, Kim Malfacini, Sam Manning, Todor Markov, Yaniv Markovskiy, Bianca Martin, Katie Mayer, Andrew Mayne, Bob McGrew, Scott Mayer McKinney, Christine McLeavey, Paul McMillan, Jake McNeil, David Medina, Aalok Mehta, Jacob Menick, Luke Metz, Andrey Mishchenko, Pamela Mishkin, Vinnie Monaco, Evan Morikawa, Daniel Mossing, Tong Mu, Mira Murati, Oleg Murk, David Mély, Ashvin Nair, Reiichiro Nakano, Rajeef Nayak, Arvind Neelakantan, Richard Ngo, Hyeonwoo Noh, Long Ouyang, Cullen O’Keefe, Jakub Pachocki, Alex Paino, Joe Palermo, Ashley Pantuliano, Giambattista Parascandolo, Joel Parish, Emy Parparita, Alex Passos, Mikhail Pavlov, Andrew Peng, Adam Perelman, Filipe de Avila Belbute Peres, Michael Petrov, Henrique Ponde de Oliveira Pinto, Michael, Pokorný, Michelle Pokrass, Vitchyr H. Pong, Tolly Powell, Alethea Power, Boris Power, Elizabeth Proehl, Raul Puri, Alec Radford, Jack Rae, Aditya Ramesh, Cameron Raymond, Francis Real, Kendra Rimbach, Carl Ross, Bob Rotsted, Henri Roussez, Nick Ryder, Mario Saltarelli, Ted Sanders, Shibani Santurkar, Girish Sastry, Heather Schmitt, David Schnurr, John Schulman, Daniel Selsam, Kyla Sheppard, Toki Sherbakov, Jessica Shieh, Sarah Shoker, Pranav Shyam, Szymon Sidor, Eric Sigler, Maddie Simens, Jordan Sitkin, Katarina Slama, Ian Sohl, Benjamin Sokolowsky, Yang Song, Natalie Staudacher, Felipe Petroski Such, Natalie Summers, Ilya Sutskever, Jie Tang, Nikolas Tezak, Madeleine B. Thompson, Phil Tillet, Amin Tootoonchian, Elizabeth Tseng, Preston Tuggle, Nick Turley, Jerry Tworek, Juan Felipe Ceron Uribe, Andrea Vallone, Arun Vijayvergiya, Chelsea Voss, Carroll Wainwright, Justin Jay Wang, Alvin Wang, Ben Wang, Jonathan Ward, Jason Wei, CJ Weinmann, Akila Welihinda, Peter Welinder, Jiayi Weng, Lilian Weng, Matt Wiethoff, Dave Willner, Clemens Winter, Samuel Wolrich, Hannah Wong, Lauren Workman, Sherwin Wu, Jeff Wu, Michael Wu, Kai Xiao, Tao Xu, Sarah Yoo, Kevin Yu, Qiming Yuan, Wojciech Zaremba, Rowan Zellers, Chong Zhang, Marvin Zhang, Shengjia Zhao, Tianhao Zheng, Juntang Zhuang, William Zhuk, and Barret Zoph. 2024. GPT-4 Technical Report. *arXiv:2303.08774 [cs.CL]*
- [26] Gaurav Parmar, Krishna Kumar Singh, Richard Zhang, Yijun Li, Jingwan Lu, and Jun-Yan Zhu. 2023. Zero-shot image-to-image translation. In *ACM SIGGRAPH 2023 Conference Proceedings*. 1–11.
- [27] Or Patashnik, Zongze Wu, Eli Shechtman, Daniel Cohen-Or, and Dani Lischinski. 2021. Styleclip: Text-driven manipulation of stylegan imagery. In *Proceedings of the IEEE/CVF international conference on computer vision*. 2085–2094.
- [28] Dustin Podell, Zion English, Kyle Lacey, Andreas Blattmann, Tim Dockhorn, Jonas Müller, Joe Penna, and Robin Rombach. 2023. Sdxl: Improving latent diffusion models for high-resolution image synthesis. *arXiv preprint arXiv:2307.01952* (2023).
- [29] Alec Radford, Jong Wook Kim, Chris Hallacy, Aditya Ramesh, Gabriel Goh, Sandhini Agarwal, Girish Sastry, Amanda Askell, Pamela Mishkin, Jack Clark, et al. 2021. Learning transferable visual models from natural language supervision. In *International conference on machine learning*. PMLR, 8748–8763.
- [30] Robin Rombach, Andreas Blattmann, Dominik Lorenz, Patrick Esser, and Björn Ommer. 2022. High-resolution image synthesis with latent diffusion models. In *Proceedings of the IEEE/CVF conference on computer vision and pattern recognition*. 10684–10695.
- [31] Chitwan Saharia, William Chan, Saurabh Saxena, Lala Li, Jay Whang, Emily L Denton, Kamyar Ghasemipour, Raphael Gontijo Lopes, Burcu Karagol Ayan, Tim Salimans, et al. 2022. Photorealistic text-to-image diffusion models with deep language understanding. *Advances in neural information processing systems* 35

- (2022), 36479–36494.
- [32] Axel Sauer, Tero Karras, Samuli Laine, Andreas Geiger, and Timo Aila. 2023. Stylegan-t: Unlocking the power of gans for fast large-scale text-to-image synthesis. In *International conference on machine learning*. PMLR, 30105–30118.
- [33] Axel Sauer, Katja Schwarz, and Andreas Geiger. 2022. Stylegan-xl: Scaling stylegan to large diverse datasets. In *ACM SIGGRAPH 2022 conference proceedings*. 1–10.
- [34] Ken Shoemake. 1985. Animating rotation with quaternion curves. In *Proceedings of the 12th annual conference on Computer graphics and interactive techniques*. 245–254.
- [35] Jiaming Song, Chenlin Meng, and Stefano Ermon. 2020. Denoising diffusion implicit models. *arXiv preprint arXiv:2010.02502* (2020).
- [36] Yang Song, Jascha Sohl-Dickstein, Diederik P Kingma, Abhishek Kumar, Stefano Ermon, and Ben Poole. 2020. Score-based generative modeling through stochastic differential equations. *arXiv preprint arXiv:2011.13456* (2020).
- [37] Hugo Touvron, Thibaut Lavril, Gautier Izacard, Xavier Martinet, Marie-Anne Lachaux, Timothée Lacroix, Baptiste Rozière, Naman Goyal, Eric Hambro, Faisal Azhar, et al. 2023. Llama: Open and efficient foundation language models. *arXiv preprint arXiv:2302.13971* (2023).
- [38] Narek Tumanyan, Michal Geyer, Shai Bagon, and Tali Dekel. 2023. Plug-and-play diffusion features for text-driven image-to-image translation. In *Proceedings of the IEEE/CVF Conference on Computer Vision and Pattern Recognition*. 1921–1930.
- [39] Clinton Wang and Polina Golland. 2023. Interpolating between images with diffusion models. (2023).
- [40] Weihao Xia, Yujiu Yang, Jing-Hao Xue, and Baoyuan Wu. 2021. Tedigan: Text-guided diverse face image generation and manipulation. In *Proceedings of the IEEE/CVF conference on computer vision and pattern recognition*. 2256–2265.
- [41] Tao Xu, Pengchuan Zhang, Qiuyuan Huang, Han Zhang, Zhe Gan, Xiaolei Huang, and Xiaodong He. 2018. Attngan: Fine-grained text to image generation with attentional generative adversarial networks. In *Proceedings of the IEEE conference on computer vision and pattern recognition*. 1316–1324.
- [42] Zhaoyuan Yang, Zhengyang Yu, Zhiwei Xu, Jaskirat Singh, Jing Zhang, Dylan Campbell, Peter Tu, and Richard Hartley. 2023. Impus: Image morphing with perceptually-uniform sampling using diffusion models. *arXiv preprint arXiv:2311.06792* (2023).
- [43] Han Zhang, Tao Xu, Hongsheng Li, Shaoting Zhang, Xiaogang Wang, Xiaolei Huang, and Dimitris N Metaxas. 2017. Stackgan: Text to photo-realistic image synthesis with stacked generative adversarial networks. In *Proceedings of the IEEE international conference on computer vision*. 5907–5915.
- [44] Han Zhang, Tao Xu, Hongsheng Li, Shaoting Zhang, Xiaogang Wang, Xiaolei Huang, and Dimitris N Metaxas. 2018. Stackgan++: Realistic image synthesis with stacked generative adversarial networks. *IEEE transactions on pattern analysis and machine intelligence* 41, 8 (2018), 1947–1962.
- [45] Kaiwen Zhang, Yifan Zhou, Xudong Xu, Xingang Pan, and Bo Dai. 2023. Diff-Morpher: Unleashing the Capability of Diffusion Models for Image Morphing. *arXiv preprint arXiv:2312.07409* (2023).
- [46] Lvmin Zhang, Anyi Rao, and Maneesh Agrawala. 2023. Adding conditional control to text-to-image diffusion models. In *Proceedings of the IEEE/CVF International Conference on Computer Vision*. 3836–3847.
- [47] Richard Zhang, Phillip Isola, Alexei A Efros, Eli Shechtman, and Oliver Wang. 2018. The unreasonable effectiveness of deep features as a perceptual metric. In *Proceedings of the IEEE conference on computer vision and pattern recognition*. 586–595.
- [48] Wenqiao Zhang, Tianwei Lin, Jiang Liu, Fangxun Shu, Haoyuan Li, Lei Zhang, He Wangui, Hao Zhou, Zheqi Lv, Hao Jiang, et al. 2024. HyperLLaVA: Dynamic Visual and Language Expert Tuning for Multimodal Large Language Models. *arXiv preprint arXiv:2403.13447* (2024).
- [49] Wenqiao Zhang, Zheqi Lv, Hao Zhou, Jia-Wei Liu, Juncheng Li, Mengze Li, Siliang Tang, and Yueting Zhuang. 2023. Revisiting the Domain Shift and Sample Uncertainty in Multi-source Active Domain Transfer. *arXiv preprint arXiv:2311.12905* (2023).
- [50] Wenqiao Zhang, Siliang Tang, Yanpeng Cao, Shiliang Pu, Fei Wu, and Yueting Zhuang. 2019. Frame augmented alternating attention network for video question answering. *IEEE Transactions on Multimedia* 22, 4 (2019), 1032–1041.
- [51] Wenqiao Zhang, Lei Zhu, James Hallinan, Shengyu Zhang, Andrew Makmur, Qingpeng Cai, and Beng Chin Ooi. 2022. Boostmis: Boosting medical image semi-supervised learning with adaptive pseudo labeling and informative active annotation. In *Proceedings of the IEEE/CVF conference on computer vision and pattern recognition*. 20666–20676.
- [52] Minfeng Zhu, Pingbo Pan, Wei Chen, and Yi Yang. 2019. Dm-gan: Dynamic memory generative adversarial networks for text-to-image synthesis. In *Proceedings of the IEEE/CVF conference on computer vision and pattern recognition*. 5802–5810.
- [53] Bhushan Zope and Soniya B Zope. 2017. A Survey of Morphing Techniques. *International Journal of Advanced Engineering, Management and Science* 3, 2 (2017), 239773.